Available online at www.sciencedirect.com
ScienceDirect
Ceramics International 36 (2010) 1845–1850
CERAMICS INTERNATIONAL
www.elsevier.com/locate/ceramint

Sintering behaviour of nanostructured glass-ceramic glazes

Julián J. Reinosa [a,*], Fernando Rubio-Marcos [a,b], Elena Solera [a], Miguel A. Bengochea [c], José F. Fernández [a]

[a] Electroceramic Department, Instituto de Cerámica y Vidrio, CSIC, C/ Kelsen 5, 28049 Madrid, Spain
[b] Departamento de Física de Materiales, UCM, 28040 Madrid, Spain
[c] Keraben S.A., Crta. Valencia-Barcelona Km 44.3, 12520 Nules, Castellón, Spain

Received 30 September 2009; received in revised form 15 February 2010; accepted 17 March 2010
Available online 26 April 2010

Abstract

The thermal behaviour of a glass-ceramic glaze based on the system SiO_2–CaO–ZnO–Al_2O_3 has been evaluated. Frit and kaolin were ball milling using dispersants and binders, and deposited on a green clay based ceramic support. The evolution of the glaze during the sintering step was observed that consisted of a glassy matrix, particles from kaolin and particles from frit. Particles from frit formed a nanostructure of interconnected nanoparticles. Pyroxenes devitrified from the glassy matrix and at higher temperatures they were dissolved in the glassy matrix. Both successes contributed to the final observed nanostructure produced by a spinodal decomposition process in which the crystalline phase had a pyroxene composition.

Keywords: A. Sintering; B. Microstructure-final; D. Glass ceramics; E. Structural applications; Pyroxenes

1. Introduction

Floor- and wall-tile ceramics are materials made from two components: the first is a support, which usually is stoneware; the second is a layer of glass which covers the substrate and provides to the whole material protection, possibilities of decoration and certain properties as erosion resistance. So certain mechanical properties are strongly influenced by the specific properties of the glaze. Mechanical, thermal and chemical properties in glass ceramics are better than in glass [1]. Abrasion resistance, impact strength, thermal sock resistance or acid and alkalis resistance are higher for glass-ceramics coatings than for glass coatings [2]. The improved properties are achieved by a controlled devitrification process that transforms the glass into a glass ceramic [3]. The stresses generated by the devitrified crystals, their size and the mean free path are responsible of the reinforcement of the glassy matrix [4].

In the last years, glass ceramics are being developed because of their importance for tiles industry. Glazes possess better performance to abrasiveness and an increased resistance compared to traditional glasses [5]. A glaze consists of both a glassy phase and different crystalline phases (i.e. anorthite, mullite or diopside) [6] to achieve the desired properties. The formation of these crystalline phases takes place according to equilibrium reactions during the firing step, and it is controlled by the total oxide composition of the glaze [7]. The amount of crystalline particles can be up to 20% in traditional matt glazes while transparent and highly glossy glazes almost entirely consist of a homogeneous glassy phase.

In general, glazes are processed from frits, kaolin and different materials as pigments. Frits are obtained by melting raw materials in a melting kiln at high temperatures ~1550 °C. The melt is cooled quickly, either by a laminating process or by quenching in water. This process transforms the obtained material into a fragmented solid that is practically insoluble in water and in the most commonly used acids and bases [8].

Tiles with improved mechanical properties and better appearance are demanded. A glazed surface is regarded as an

* Corresponding author at: Ceramics for Smart Systems Group, Electroceramic Department, Instituto de Cerámica y Vidrio, CSIC, C/ Kelsen 5, 28049 Madrid, Spain. Tel.: +34 91 735 5840x1080; fax: +34 91 735 5843.
E-mail address: jjreinosa@icv.csic.es (J.J. Reinosa).

0272-8842/$36.00
doi:10.1016/j.ceramint.2010.03.029

easy-to-clean surface. However, during its applications, glazes suffer several deteriorations as: surface pitting; lost of brightness and colour and the decrease of the cleanability because surface roughness increases and the close porosity of the glaze opens [9].

The main glass-ceramic material is known as Silceram, composed by $CaO–MgO–Al_2O_3–SiO_2$ and originally designed for application as erosion and abrasion resistant materials at room temperatures [10]. It was reported that glazed tiles developed from compositions in this ternary system present higher abrasion strength and gloss. From this composition, new systems as $CaO–MgO–SiO_2$ or $Li_2O–CaO–MgO–Al_2O_3–SiO_2$ were studied [10]. The aim of this work is to evaluate the thermal behaviour of a glaze used for transparent and glazy glazes for tiles based on the system $SiO_2–CaO–ZnO–Al_2O_3$, which shows a crystalline phase evolution and a nanostructure similar to diopside.

2. Experimental procedure

To obtain the ceramic glaze, frit and kaolin powders with ratio 91/9 in weight were ball milled for 20 min in a porcelain jar with alumina balls, using water as 33 wt% and 0.1 wt% of sodium tripolyphosphate as a dispersant and 0.3 wt% of carboximethyl cellulose as a binder. After milling, to achieve a more dispersed suspension [11], a turbine of high speed of shears was used and the mix was left in rest for 4 h to eliminate bubbles. According to the chemical composition (Table 1), the main components of the glaze starting composition expressed as oxides were SiO_2, CaO, ZnO, Al_2O_3, K_2O and B_2O_3. In this study, a glaze layer was deposited on a green clay based ceramic support of stoneware by means of a waterfall casting system to obtain a homogenous layer of ~300 μm in thickness. Porcelain stoneware is a densify material (water absorption <0.5%) made of quartz, feldspar and clay principally [12]. After oven drying, the stoneware tiles with the deposited glaze were fired in a laboratory electrical furnace in only one sintering process. This process is characterized by a simulated industrial cycle that consists of a fast firing process in air atmosphere involving basically: an average heating rate of 26 °C/min, a soaking temperature of 1140 °C hold 6 min and a furnace cooling step.

Table 1
Chemical composition of the glaze powder, determined by XRF.

Compound	wt%
B_2O_3[a]	2.9 ± 0.1
Al_2O_3	9.0 ± 0.1
SiO_2	59.1 ± 0.3
K_2O	3.52 ± 0.05
CaO	12.7 ± 0.2
Fe_2O_3	0.25 ± 0.03
Na_2O[b]	0.05 ± 0.01
SrO	0.07 ± 0.01
SO_3	0.06 ± 0.01
P_2O_5	0.11 ± 0.02
ZrO_2	0.13 ± 0.02
PbO	0.13 ± 0.02
ZnO	10.98 ± 0.02
MgO	1.01 ± 0.04

[a] Volumetry.
[b] AA.

In addition, in order to study the effect of the crystalline phases growth, a second sintering cycle modifying the mentioned one was realized. Therefore a second soak temperature at 950 °C for 1 min and 1 h was introduced in the simulated industrial sintering cycle.

The glaze powder was characterized by chemical analysis which was carried out using two techniques: atomic absorption to determine alkaline elements by a PerkinElmer 2100 Spectrophotometer and X-ray florescence analysis using a Magic X Phillips Spectrophotometer.

Thermal behaviour of the glaze was studied by means of differential thermal (TDA) and thermogravimetric (TG) analysis using a Thermo-Analizer Netzch STA 409 with a temperature controller Netzch TASC 414/2 being the reference α-Al_2O_3. Hot-stage microscopy was carried out in the range 30–1200 °C with a heating rate of 20 °C/min by a Leica Leitz microscope.

The viscosity curve for the glaze was determined by a fast process known as the three points method that consist of the resolution of the Vogel–Fulcher–Tamman's equation (Eq. (1)) using three values of viscosity–temperature [13,14] where A, B and T_0 are constants which do not depend on temperature.

$$\log \eta = A + \frac{B}{T - T_0} \quad (1)$$

After sintering the glaze were characterized by X-ray diffraction analysis which was performed using a graphite monochromatic CuK_α radiation and a Ni filter, operating at 50 kV, 30 mA and a scanning rate of 0.02°/min, using a Siemens D500 Diffraktometer.

Sintered tiles were polished and then etched chemically with HF at 25 vol.%, and gold coated for microstructure analysis. The microstructure was studied by a Field Emission Scanning Electron Microscope FE-SEM, Hitachi S-4700, equipped with an energy dispersion X-ray analysis and EDS, using a resolution of 1.5 nm at 15 kV.

3. Results and discussion

Fig. 1 shows the DTA/TG curves recorded for the glaze powders. The first weight lost observed was related to the exothermic removal of organic compounds such as carboximethyl cellulose and the organic material in the clays [15]. The second weight lost, ~515 °C, was attributed to the endothermic

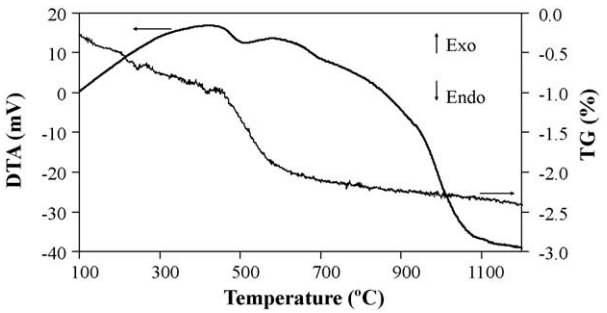

Fig. 1. DTA and TG curves of glaze.

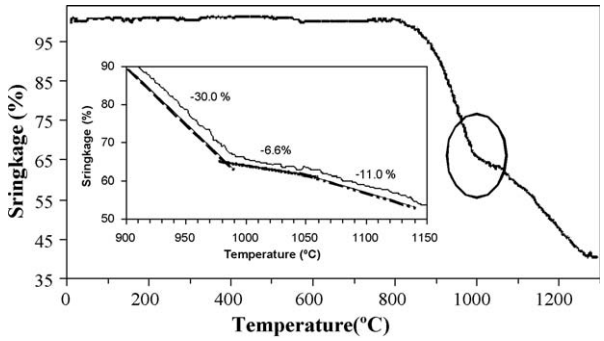

Fig. 2. Glaze shrinkage behaviour vs sintering temperature. The inserted shows detail of the shrinkage curve. The different slopes were calculated to be compared (dotted lines in the insert graph).

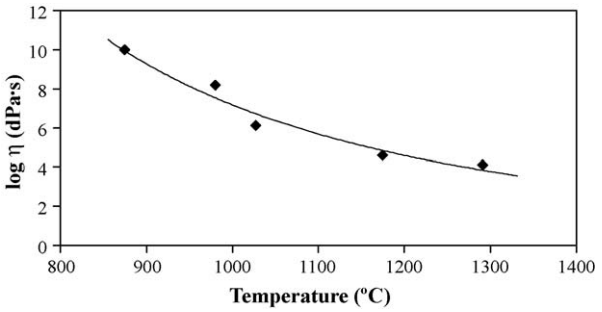

Fig. 4. Glaze curve viscosity calculated by the tree points method. The solid line shows the expected tend.

dehydroxylation of the kaolinitic clay to produce the metakaolinitic clay [16]. Finally a large decrease of the base line is observed from ∼900 °C without a significant weight lost which is related to a large decreased of the density of the powders. The absence of the transformation of metakaolin to spinel phase is due to the reaction of the metakaolin with the matrix. It was reported that the presence of glass forming cations reduces the temperature at which the exothermic pick of the transformation of metakaolin to spinel takes place [17], but in the present case the metakaolin reacted with the matrix previously and this transformation was avoided.

Fig. 2 shows the shrinkage curve of the glaze powder which was determined from the hot-stage microscopy. At ∼550 °C a small shrinkage related to the dehydroxylation of the kaolin was observed. The glaze shrunk between 800 °C and ∼1300 °C and different slopes of the shrinkage curve were observed. At ∼800 °C the glaze powders started to shrink with a low rate, indicating a mechanism associated with low mass transport due to the reaction of the metakaolin with the particles of frit. For temperatures >900 °C the slope of the shrinkage curve increased largely due to liquid phase appearance. The sintering rate was reduced at ∼1000 °C and required to increase the temperature >1050 °C to reach a high sintering rate again.

The most characteristic temperatures of the glaze during the firing process are shown in Fig. 3. At 875 °C the beginning of the sintering step of the glaze took place and the maximum shrinkage point before softening was reached at 980 °C. This point could be related to the change of the slope in the DTA curve at the same temperature. Total softening occurred at 1027 °C being the middle burble point at 1174 °C. Finally, the glaze fluxed from 1291 °C. The appearance of liquid at >500 °C is thus limited and it was related to the reaction of metakaolin with the glass forming cations of the frit. This liquid was rapidly consumed and before the total softening the liquid changed in composition because of the reaction.

The viscosity curve, which was calculated by Eq. (1) from the hot-stage microscopy curve, is shown in Fig. 4. The constants obtained for the viscosity curve from the mentioned points did not depend on the temperature, and their calculated values were $A = -1.56$, $B = 5189$ and $T_0 = 512$ °C. Paying attention to the viscosity curve, the viscosity decreased with an increase of the temperature during the sintering, as a normal ceramic glaze, but near 980 °C (temperature of maximum contraction before softening) a deviation in the tendency of the viscosity occurred. This fact means that higher temperature is need to reach the softening point. So the increase of the viscosity was thus on the origin of the sintering reduction and it could be related to the liquid composition change or to a microstructural evolution.

XRD patterns of ceramic glaze fired at 950 °C (temperature previous to the variation in the viscosity curve) for 1 min and 1 h were performed in order to investigate the nature of the crystalline phases (Fig. 5). The XRD pattern shows a wide band corresponding to the glassy matrix and diffraction peaks associated to the different crystalline phases. For the 1 min fired sample the crystalline phase was identified as anorthite (ICSD Card 081450) associated to the kaolinitic clay [18], which confirmed that the metakaolin reacts with the glassy matrix during the earliest stage of the sintering step. In the same study for 1 h fired glaze were evidenced two phases: anorthite, $CaAl_2Si_2O_8$, and diopside, $CaMgSi_2O_6$. Both of them are widely spread in nature and belong to the plagioclase

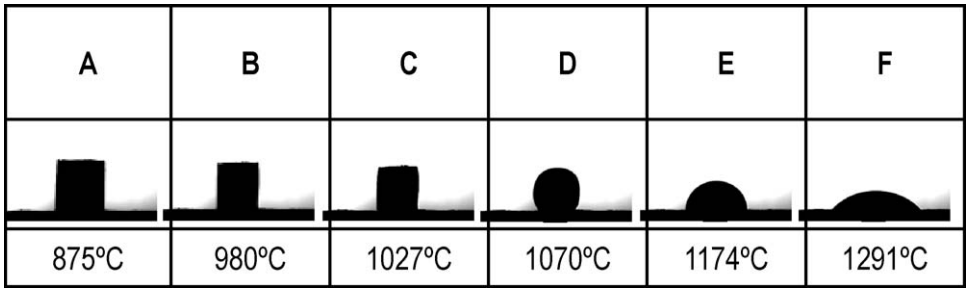

Fig. 3. Temperatures at which the main processes take place during the sintering of the glaze.

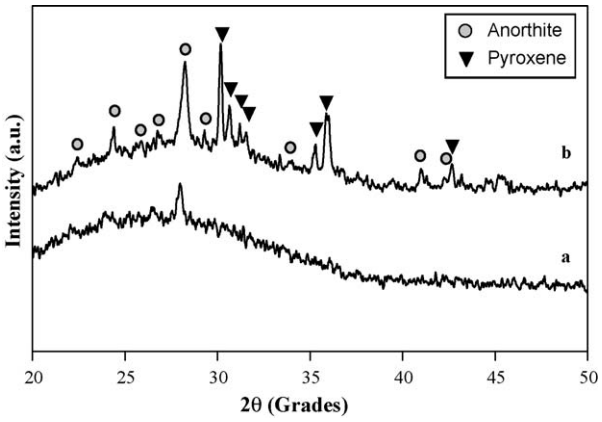

Fig. 5. (a) XRD patterns of ceramic glaze fired at 950 °C for 1 min and (b) for 1 h.

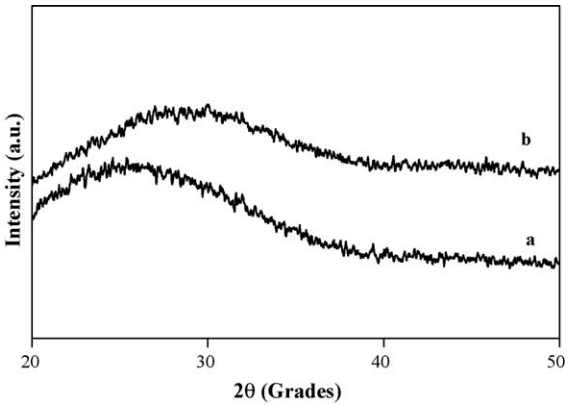

Fig. 6. (a) XRD patterns of ceramic glaze fired at 1140 °C for 1 min and (b) for 1 h.

and pyroxene group of rocks forming minerals [19]. Meanwhile the anorthite comes from the kaolinitic clay; the diopside seems to be related to the spinel decomposition of the frit particles.

Previous XRD studies [20] suggested that bands of akermanite ($Ca_2MgSi_2O_7$) appear together with diopside ones, but some authors [21] reported that gahnite ($ZnAl_2O_4$) bands are coincident with akermanite and diopside too. In addition, it was found that in compositions with low concentration of alkalis and high concentration of iron only two phases (anorthite and diopside) appeared because diopside is promoted by impurities of Fe_2O_3 [20]. All of them have the same microstructure and their diffraction peaks are coincident so it is difficult to establish differences between the mentioned phases; for this reason, the best way to address these crystalline phases is under the general name of pyroxenes (ICSD Card 022022) [10], which are built on single tetrahedral SiO_4 chains. Actually, ceramics and glass ceramics based on pyroxenes attract increasing interest in several advanced fields, such as electronics or immobilization of radioactive wastes [22]. It has been studied that cations as Na^+, K^+, Ti^{4+} and B^{3+} favour the crystallization of crystalline phases with structure of pyroxene because they form part of pyroxene crystals. In addition these cations decrease the liquid viscosity and facilitate the solid solution formation [1]. The devitrification process of the pyroxene possessed a composition base similar to the composition inside of frit grains. Thus, this is the mechanism that increased the viscosity and reduced the sintering rate because of the nanocrystalline appearance. A high amount of crystalline phases had a positive effect on the mechanical properties, as reported before [1,23,24].

XRD patterns of the glazes at 1140 °C (point of maximum heating) were studied for 1 min and 1 h to be sure of the total dissolution of the crystalline phases. As it can be seen in Fig. 6, both XRD patterns show a wide band corresponding with the glass matrix and the absence of relevant diffraction peaks. The difference in the displacement of the wide band to higher angle in 1 h sample is attributed to the approaching of the ions between them in glass matrix and is related to a higher stress of the glass matrix.

Crystallizations as nanospherical phase of pyroxene were presented in the glaze in the final product, after an industrial standard sintering process, as it can be seen in Fig. 7. It indicated that the process of devitrification of pyroxenes and the segregation of ions from the matrix to generate crystalline particles took place also during the cooling step. The pyroxene nanocrystalline phase is homogeneously distributed along the whole glaze thanks to higher temperature and to the homofunctionalization of the glaze due to the spinodal decomposition process during cooling (Fig. 7). Thus, the higher temperature consolidated a homogeneous glassy matrix that devitrified during the cooling step. The nanosize of the crystalline phase, <100 nm, is quite below to the visible wavelength so the result is a transparent glossy glaze. The higher mechanical properties of the glazes when are compared with usual glasses could be attributed thus to the presence of crystalline phases [1,22,23], in this case to a nanocrystalline pyroxene matrix.

To determinate the nature of the crystallizations, the glaze was treated thermally at 950 °C during sintering times between 1 min and 1 h, in order to effectively promote the growth of the nanocrystals (Fig. 8a–c). The crystalline phases were observed by the FE-SEM analysis. For a very short holding time, 1 min at

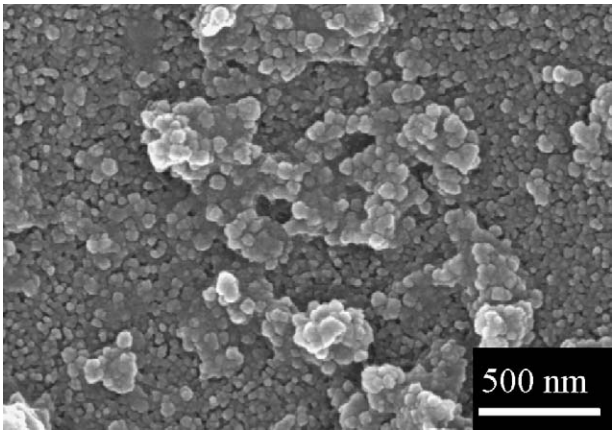

Fig. 7. SEM micrograph of the structure of the sintered glaze in the final product sintered as standard sintering cycle: detail of the pyroxenes nanostructure due to the spinodal decomposition mechanism.

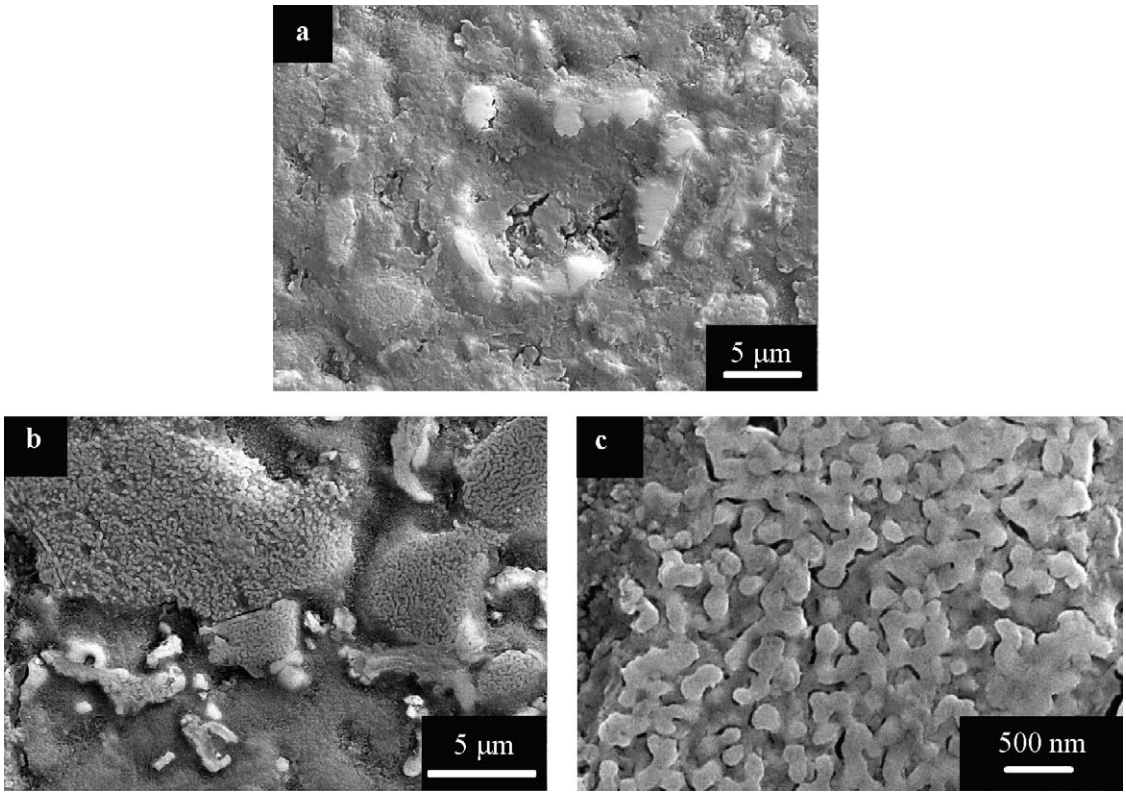

Fig. 8. SEM micrographs corresponding to the microstructure of the fired glaze at 950 °C. (a) 1 min: crystalline particles and devitrification of pyroxenes. (b) 1 h: evidence of the three components in the glaze: crystalline anorthite particles, devitrification of pyroxenes and glassy matrix. (c) 1 h: detail of the pyroxenes nanostructure due to spinodal decomposition mechanism.

950 °C (see Fig. 8a), a complex microstructure may be recognised, as observed in the backscattered image. It consisted on glassy matrix, a small layered particles corresponding to anorthite and irregular big particles formed by pyroxenes. Meanwhile, for a longer soaking time, 1 h, it was caused a very widespread crystallization inside the big particles (see Fig. 8b). The formation of irregular big particles can be attributed to the devitrification mechanism. Within the large particles it can be observed more in detail the nanocrystals emerging (Fig. 8c). The small nanoparticles-crystals forming the irregular big particles reasonably correspond to pyroxenes developed from the surface of the glassy matrix because of the presence of iron [25], as it was confirmed by XRD (Fig. 5). This microstructure of particles forming an interconnected 3D network is typical of spinodal decomposition [26].

4. Conclusions

The chemical behaviour for crystalline ceramic glaze has been studied and a devitrification process has been observed, taking place the formation of crystalline nanoparticles with pyroxene structure. This structure is generated during the sintering process as a devitrification of the pyroxene and during the cooling of the ceramic glaze so the procedure is inherent to the composition.

The presence of anorthite (due to kaolinitic clay) in the glaze sets the liquid phase and increases the viscosity locally, inhibiting the elimination of porosity. At the point of maximum softening the viscosity increases respect to the trend curve; this fact corresponds with the devitrification of the glassy phase that has nanometric particles of pyroxene as a result.

Acknowledgments

The authors thank to the projects MAT2007-66845-C02-01 and CENIT DOMINO by the financial support. Dr. F. Rubio-Marcos thanks the FPI-CAM-FSE program for the research grant.

References

[1] F.J. Torres, J. Alarcón, Mechanism of crystallization of pyroxene-based glass-ceramics glazes, J. Non-Cryst. Solids 347 (2004) 45–51.
[2] A. Majumdar, S. Jana, Glass and glass-ceramic coatings, versatile materials for industrial and engineering applications, Bull. Mater. Sci. 24 (1) (2001) 69–77.
[3] Cer-glas, Chemical resistance and cleanability of glazed surfaces. Surface science, Bol. Soc. Esp. Ceram. V 33 (2) (1994) 99–102.
[4] D.I.H. Atkinson, P.W. McMillan, Floor tile glass-ceramic glaze for improvement of glaze surface properties, J. Mater. Sci. 11 (6) (1976) 994–1002.
[5] C. Lira, A.P. Novaes de Oliveira, O.E. Alarcón, Sintering and crystallisation of $CaO–Al_2O_3–SiO_2$ glass powder compacts, Glass Technol. 42 (3) (2001) 91–96.
[6] B.E. Yekta, P. Alizadeh, L. Rezazadeh, Glass-ceramics with random and oriented microstructures. Part 2. The physical properties of a randomly oriented glass-ceramic, J. Eur. Ceram. Soc. 26 (2006) 3809–3812.

[7] L. Hupa, R. Bergman, L. Fröberg, S. Vane-Tempest, M. Hupa, T. Kronberg, E. Peisonen-Leinonen, A.-M. Sjöberg, Chemical resistance and cleanability of glazed surfaces, Surf. Sci. 585 (2005) 113–118.
[8] C. Gonzlavo, M. Molina, The manufacture of frits, glazes and ceramic colours: social, economic and environmental challenges in the international context, in: Proceedings of the X World Congress on Ceramic Tile Quality Qualizer, Castellón, Spain, February 13–15, 2006.
[9] M.G. Rasteiro, T. Gassman, R. Santos, E. Antunes, Crystalline phase characterization of glass-ceramic glazes, Ceram. Int. 33 (2007) 345–354.
[10] F.J. Torres, J. Alarcón, Pyroxene based glass ceramics as glazes for floor tiles, J. Eur. Ceram. Soc. 25 (2005) 349–355.
[11] E. Solera, J.F. Fernández, M.A. Bengochea, C. Fernández, High-shear dispersion of screen-printing inks, Am. Ceram. Soc. Bull. 12 (2004) 9201–9204.
[12] P.M. Tenorio Cavalcante, M. Dondi, G. Ercolani, G. Guarini, C. Melandri, M. Raimondo, E. Rocha e Almendra, The influence of microstructure on the performance of white porcelain stoneware, Ceram. Int. 30 (2004) 953–963.
[13] J.M. Fernández Navarro, Glass (El Vidrio), Sociedad Española de Cerámica y Vidrio & Consejo Superior de Investigaciones Científicas, Madrid, Spain, 1991, p. 341.
[14] M.J. Pascual, M.O. Prado, A. Durán, A new method for determining fixed viscosity points of glasses, Phys. Chem. Glasses 46 (2005) 512–520.
[15] C. Lii, P. Tomaski, H. Zaleska, S. Liaw, V.M.F. Lai, Carboximethyl cellulose–gelatin complexes, Carbohyd. Polym. 50 (2002) 19–26.
[16] K.D. Swapan, D. Kausik, Differences in densification behaviour of K-and Na-feldspar-containing porcelain bodies, Thermochim. Acta 406 (2003) 199–206.
[17] L. Carbajal, F. Rubio-Marcos, M.A. Bengochea, J.F. Fernández, Properties related phase evolution in porcelain ceramics, J. Eur. Ceram. Soc. 27 (2007) 4065–4069.
[18] Y. Kobayashi, E. Kato, Low-temperature fabrication of anorthite ceramics, J. Am. Ceram. Soc. 77 (3) (1994) 833–834.
[19] V.M.F. Marques, D.U. Tulyaganov, S. Agathopoulos, J.M.F. Ferreira, Low temperature production of glass ceramics in the anorthite-diopside system via sintering and crystallization of glass powder compacts, Ceram. Int. 34 (2008) 1145–1152.
[20] D.U. Tulyaganov, M.J. Ribeiro, J.A. Labrincha, Development of glass ceramics by sintering and crystallization of fine powders of calcium-magnesium-aluminosilicate glass, Ceram. Int. 28 (2002) 515–520.
[21] C. Wu, J. Chang, Synthesis and apatite formation ability of akermanite, Mater. Lett. 58 (2004) 2415–2417.
[22] A. Goel, D.U. Tulyaganov, S. Agathopoulos, M.J. Ribeiro, J.M.F. Ferreira, Crystallization behaviour, structure and properties of sintered glasses in the diopside–Ca–Tschermak system, J. Eur. Ceram. Soc. 27 (2007) 3231–3238.
[23] E. Bernardo, L. Esposito, E. Rambaldi, A. Tucci, Y. Ponikes, G.N. Angelopoulus, Sintered esseneite-wallastonite-plagioclase glass-ceramics from vitrified waste, J. Eur. Ceram. Soc. 29 (2009) 2921–2927.
[24] F. Lucas, A. Belda, F.J. Torres, J. Alarcón, Estudio y caracterización de vidriados vitrocerámicos basados en piroxeno, Bol. Soc. Esp. Ceram. V. 43 (2004) 849–854.
[25] W. Höland, G. Beall, Glass-Ceramics Technology, The American Ceramics Society, Westerville, OH, USA, 2002.
[26] Zarzycki, Glass and the Glassy State,(Les Verres et l'Etat Vitreux), Masson, Paris, 1982.